TRIUMF — RESEARCH PROPOSAL		Experiment no.	Sheet 1 of 34
		952	

Title of proposed experiment:

$^{12}C(\alpha,\gamma)^{16}O$ at DRAGON

Name of group: Cargontag

Spokesperson for group: L.Buchmann

E-Mail address: lothar@triumf.ca **Fax number:** 604-222-1074

Members of the group (name, institution, status, per cent of time devoted to experiment)

C. Barbieri	TRIUMF	Research Associate	30%
C.R. Brune	U. of Ohio	Assistant Professor	20%
L. Buchmann	TRIUMF	Senior Research Scientist	30%
A. Chen	McMaster University	Assistant Professor	10%
J. D'Auria	SFU	Professor	10%
J. Görres	U. of Notre Dame	Research Professor	10%
U. Greife	Colorado School of Mines	Assistant Professor	10%
A. Hussein	University of Northern British Columbia	Professor	20%
D. Hutcheon	TRIUMF	Senior Research Scientist	20%
A.M. Laird	TRIUMF	Research Associate	10%
Z. Li	Chinese Institute of Atomic Energy	Research Associate	40%
A. Murphy	U. of Edinburgh	Research Associate	30%
S. Park	TRIUMF	Research Associate	30%
J. Rogers	TRIUMF	Senior Research Scientist	30%
F. Sarazin	TRIUMF	Research Associate	30%
J.M. Sparenberg	TRIUMF	Research Associate	30%
M. Wiescher	U. of Notre Dame	Professor	20%
S. Woosley	U.C. Santa Cruz	Professor	5%

Start of preparations:	now	Beam time requested:		
		12-hr shifts	Beam line/channel	Polarized primary beam?
Date ready:	now	30/100	ISAC-HE/DRAGON	na
Completion date:	2006			

The stellar reaction rate of the ^{12}C$(\alpha,\gamma)^{16}$O reaction is the most important one yet to be determined in Nuclear Astrophysics. Since DRAGON is the only operational recoil separator where signals of ^{12}C$(\alpha,\gamma)^{16}$O can be detected both as γ-ray emission as well as the recoiling ^{16}O, it is proposed to measure the ^{12}C$(\alpha,\gamma)^{16}$O reaction cross section at the DRAGON facility encompassing both the measurement of ground state as well as cascade transitions from 2 MeV to 6.5 MeV (cm). It has been shown in particular that the measurement of the 6.9 MeV cascade transition is directly related to the E2 strength of the ground state transition which measurement will therefore be the main emphasis of the experiment. At the same time, the ground state transition can be measured over a wide range of energies shedding light on some of the γ interference signs necessary to be known in ^{12}C$(\alpha,\gamma)^{16}$O. Angular distributions will be measured both in the recoil and the γ-detectors. A statistical error of S_{E2} (300) of the order of 10% of the E2 ground state transition is feasible in this experiment while the uncertainties in other transitions should be greatly reduced. New theoretical approaches as alternatives to extrapolations by R-matrix theory will be explored, in addition.

Experimental area

    ISAC-HE, DRAGON

Primary beam and target (energy, energy spread, intensity, pulse characteristics, emittance)

    ^{12}C stable, 0.5-1.64 MeV/u, 1pμA and more

Secondary channel   none

Secondary beam (particle type, momentum range, momentum bite, solid angle, spot size, emmittance, intensity, beam purity, target, special characteristics)

    none

TRIUMF SUPPORT:

Gas stripper after RFQ
Operational support

NON-TRIUMF SUPPORT

We have most of the equipment on-site. Two large volume germanium detectors need to be found (either TIGRESS detectors, separate NSERC application, or outside collaborators). A quadrupole doublet has to be built into the gas target, funding will be sought from NSERC.

The reaction rate of ^{12}C$+\alpha$ is notoriously low and the beam is stable. The gas target operates with helium.

1 Scientific Justification

1.1 Introduction

For anyone who ever followed a Nuclear in the Cosmos symposium, trying to improve the accuracy of the $^{12}C(\alpha,\gamma)^{16}O$ stellar reaction rate does not require any justification. For those who didn't have the pleasure, the justification is given below. Without a shred of doubt, however, it can already be stated that a better determination of the $^{12}C(\alpha,\gamma)^{16}O$ reaction rate is the most important experiment ever to be performed in the nuclear astrophysics program at ISAC.

The stellar rate of quiescent helium burning for the $^{12}C(\alpha,\gamma)^{16}O$ reaction is one of the great unknowns left in Nuclear Astrophysics. Its importance to stellar modeling arises from the fact that the $^{12}C(\alpha,\gamma)^{16}O$ reaction in the helium core of a star takes place simultaneously with the triple α reaction. For a given thermal environment, the ratio of these two reactions is fixed in contrast to other burning stages of a star where only the flow through one reaction is hydrodynamically important. Such a single reaction flow can then be easily adjusted by minor changes e.g. in temperature. In contrast to such a situation the ratio of carbon and oxygen at the end of the helium burning phase of stellar evolution is given solely by the ratio of the stellar reaction rates of radiative α capture on ^8Be and ^{12}C. Experimentally allowed variations in this ratio for different mass stars lead then to quite different developmental paths later on and final element production. For an understanding of the evolutionary changes of a massive star caused by varying the $^{12}C(\alpha,\gamma)^{16}O$ rate see Ref. [1] which has updated information from Ref. [2].

For stars lower than eight solar masses stellar evolution will lead to a C/O white dwarf. Its mass/radius composition will again depend on the $^{12}C(\alpha,\gamma)^{16}O$ reaction rate. This is particularly important if the white dwarf happens to be the progenitor of a SNIa, setting this way the initial condition for the explosion. Supernovae of type Ia are now widely used as cosmological standard candles but are still requiring a better theoretical understanding.

The difficulties in determining this rate of $^{12}C(\alpha,\gamma)^{16}O$ for quiescent helium burning, which typically takes place around center-of-mass-energies of 300 keV, comes experimentally from the fact that the cross section is very small ($\approx 10^{-17}$ b) and could not be determined by direct measurements so far. The extrapolation to low energies is difficult as the cross section in this energy region is a mixture of groundstate and cascade transitions from resonant tails with no (natural parity) state in ^{16}O for astrophysically relevant energies. The cross section of the groundstate transitions is indeed dominated by the tails of subthreshold resonances (-45 and -245 keV[1]) in this energy region with other processes interfering. Cascade transitions, believed smaller in cross section, are dominated by direct or resonance processes. While radiative widths of states in ^{16}O are often well known, it is in general the α-widths of states, in particular those below the $^{12}C+\alpha$ threshold, which cause the problems in predicting the stellar rates of $^{12}C(\alpha,\gamma)^{16}O$ at low energies. In principle, α-widths which are common to all possible radiative decays, can be determined in elastic scattering or other methods which should have, if applied, the advantage that high statistical accuracy can be obtained with minimum effort. Therefore the main thrust in such an experiment involving indirect methods has to be directed to minimize systematic

---

[1]If not otherwise noted, energies are in the centre-of mass system of ^{12}C and α.

problems. In fact, even with proposals around to drive direct $^{12}C(\alpha,\gamma)^{16}O$ measurement down to E=700 keV, extrapolation will still be necessary, and it can be shown that reasonably small restrictions of S(300) can only be achieved applying indirect restrictions to α-widths simultaneously [3].

The α-width of the 7.117 MeV $J^\pi=1^-$ state in ^{16}O (E=−45 keV) has been restricted by measuring the β-delayed α-spectrum of ^{16}N [4]. Such a measurement is in principle similar to an elastic scattering experiment. However, because of the β-branching ratio of 10^4 preference for the population of the 7.1 MeV subthreshold state, the influence of the subthreshold state is highly amplified in the ^{16}N spectrum. The result on the α-width leads to a reasonable restriction in the $E1$ radiative capture cross section, though further improvements are necessary to reach the level of 20% error at 2σ as demanded by stellar modelers [5]. Below, we will present an equivalent method to restrict the $E2$-part of the groundstate transition by determining the α-width of the 2^+ ground state transition by employing the cascade transition through this state. Properties of cascade transitions may, in addition, be derived reasonably well from direct and indirect measurements in this experiment.

1.2 Recent results from an elastic scattering experiment

In a recent $^{12}C+\alpha$ elastic scattering experiment at Notre Dame University [6], the following conclusions were drawn using the R-matrix formalism outlined below: the best fit for the reduced width amplitude[2] of the 2^+ sub-threshold state ($E_x=6.917$ MeV[3], E=−245 keV) occurred for $\gamma_{12}=0.47$ MeV$^{1/2}$, with $\gamma_{11}=0.27$ MeV$^{1/2}$ for the sub-threshold 1^- state ($a=5.5$ fm). To obtain an error estimation, fits were obtained for values of γ_{12} from 0.2 to 0.60 MeV$^{1/2}$, with all other parameters being allowed to vary. The same approach was used to scan γ_{11} from 0 to 0.60 MeV$^{1/2}$ for the 1^- state. A 1σ uncertainty of $\gamma_{12}=0.47\pm0.06$ MeV$^{1/2}$, and $\gamma_{11}=0.27^{+0.11}_{-0.27}$ MeV$^{1/2}$ was calculated with the previously established [4] guideline $\chi^2 < \chi^2_{min} \pm 9\chi^2_\nu$. This has to be compared to $\gamma_{11}=0.18\pm0.02$ MeV$^{1/2}$ of Ref. [4]. The best fit has a χ^2_ν of approximately 1.66. Deviations from an ideal fit occurred at resonances with widths in the keV range where the sensitivity to target effects and beam energy calibration was most pronounced.

The influence of the interaction radius[4] a on the results has been also investigated in Ref. [6] using elastic scattering data. A strong dependence of the least squares parameter χ^2 as a function of a was found with $a=5.42^{+0.16}_{-0.27}$ fm as the best value. The width γ_{12} decreases, as expected, with increasing a. Close to the minimum an approximate $\frac{1}{a}$ dependence is found for γ_{12} and other widths. This result justifies using $a=5.5$ fm throughout the discussion below and represents the first real restriction on the interaction radius a in the $^{12}C(\alpha,\gamma)^{16}O$ problem which has some immediate consequences as discussed in Sec. 1.4.1.

---

[2]For R-matrix notations, see Ref. [3,4] and references therein, see also appendices 1 and 2. The reduced width amplitude γ_{12} is a measure of the the α width of a state. The indices 12 indicate the first state of angular momentum two, i.e., the 6.9 MeV state in ^{16}O. S(300) of the ground state transition scales approximately with the square of the reduced width amplitude.

[3]For conciseness in the subsequent text, state energies will be truncated to two significant figures and may be used as indices for symbols, e.g. $\theta_\alpha^{6.9}$.

[4]The interaction radius a is the size of the square potential in R-matrix theory. It is, in principle, a free parameter though somewhat constrained by nuclear theory and reason.
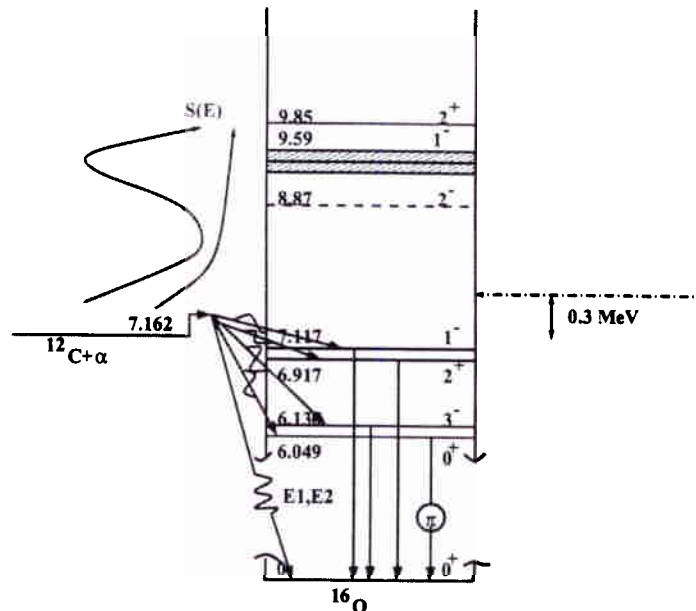
Fig. 1 Radiative capture scheme for ^{12}C+α. The position of the astrophysically most important energy of 300 keV is shown as well as a crude representation of the $E1$ and $E2$ radiative ground state S-factors.

1.3 The γ-ground state transition

1.3.1 Angular distributions and E1 transitions

In the measurement of the ^{12}C$(\alpha,\gamma)^{16}$O reaction several γ-decays are observed, as shown in Fig. 1. They can be roughly named cascade (2 γ-rays) and ground state (1 γ-ray) transitions. The ground state transitions are by far the dominant in cross section, largely because of the power of energy dependences of radiative transitions.

For the ground state, only $E1$ and $E2$ radiative capture is allowed (see, however, Sec. 1.5 about ground state E0 transitions). They mix in the angular distributions following Eq. 5 (Sec. 6.1, Appendix1), while they add up incoherently in the total cross section. The way to distinguish both transitions experimentally is either to measure γ angular distributions and evaluate Eq. 5, or for the $E1$ transition to measure at 90° only.

From $E1$ data derived this way and fitting simultaneously using Eq. 7 and Eq. 8 for the radiative capture and Eq. 9 (Sec. 6.1, Appendix 1) for the ^{16}N β-delayed α-spectrum one obtains an extrapolation of the cross section to an energy of 300 keV as shown in Fig. 2. The $E1$ cross section in the low energy region as shown in Fig. 2 is largely the result of the two interfering 1$^-$ states of 7.12 and 9.6 MeV in ^{16}O. For E=300 keV the subthreshold 1$^-$ state is dominant. The result of this fit is $S_{E1}(300)$=80±20 keV b [4].

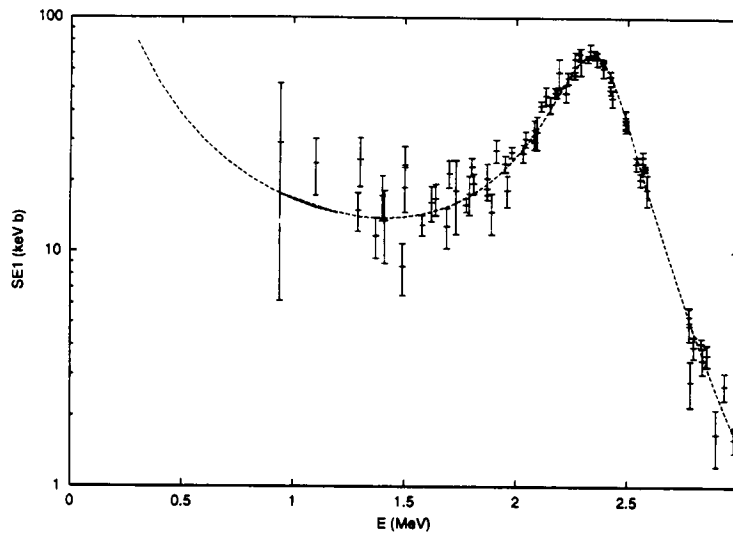Fig. 2 The $E1$ S-factor of $^{12}C(\alpha,\gamma)^{16}O$ obtained in a simultaneous fit to the ^{16}N spectrum.

1.3.2 The $^{12}C(\alpha,\gamma)^{16}O$ $E2$ case

Because of the existence of the 1^- state at $E=2.4$ MeV, the influence of the E2 radiative capture on measurements in this energy region is weaker. The cross section in the energy range of the data is largely $E2$ direct capture to the ^{16}O ground state, while the S-factor at 300 keV results mostly from the 6.92 MeV subthreshold state in ^{16}O. Restrictions are not very stringent on $S_{E2}(300)<140$ keV b for using radiative capture alone [3].

Previous extrapolations of $S_{E2}(300)$ have been made using simultaneous fits to all available primary data [3]. Direct inclusion of all the elastic scattering data discussed above (Sec. 1.2) will, however, statistically dominate other data sets. For this reason, the reduced width amplitude γ_{12} can be directly fixed within its errors in such fits without significantly narrowing the χ^2 range estimated in the minimization. Therefore the best-fit elastic scattering parameters for the 2^+ states can be combined with radiative capture data [8–11] from $^{12}C(\alpha,\gamma)^{16}O$ and ^{16}N data [4]. This analysis (Sec. 1.2 and Ref. [6]) leads to a value of $S_{E1}(300)=80\pm20$ keV b, and $S_{E2}(300)=49^{+7}_{-9}$ or 58^{+8}_{-11} keV b, depending on the sign of the $E=4.36$ MeV 2^+ resonance γ width amplitude relative to that for direct capture and the subthreshold resonance (see Sec. 1.5). As this interference sign is unknown, the two results are averaged and errors include the limits on both measurements, yielding $S_{E2}(300)=53\pm13$ keV b. With the full range of a allowed covered (see above), the final result of the elastic scattering experiment is $S_{E2}(300)=53^{+13}_{-18}$ keV b [6]. In this analysis destructive interference between the ground state direct capture and the tail of the subthreshold 2^+ resonance has been employed. This is justified by a total decrease in χ^2 of nearly 300 between the destructive and constructive option resulting largely from the γ-angular distributions of Refs. [9] and [11]. However, additional angular distributions would be desirable, as the constructive option leads to 92 and 102 keV b, respectively, for $S_{E2}(300)$. The data set of Ref. [12] are unfortunately not available to improve the analysis. The aim of the ground state transition experiment is therefore to shed some light onto these interference signs.

1.4 The importance of cascade transitions

1.4.1 The cascade through the 6.9 MeV state

The following section is largely a copy of an article [13], proposing to measure the γ-cascade through the 6.9 MeV 2^+ state to directly conclude the reduced α width of this state. This indirect approach to $S_{E2}(300)$ is the mainstay of the present proposal.

Relatively little attention has been paid to the cascade transitions in the $^{12}C(\alpha,\gamma)^{16}O$ reaction. Existing data [7,9] show that their contribution is likely of the order of 10% of the total cross section at astrophysically important energies. However, the theoretical descriptions of the cross section for cascade and ground state transitions are closely related. For the dominant cascade transition through the subthreshold 6.9 MeV $J^\pi=2^+$ state [14], the cross section is largely governed by the direct capture process, also known as nonresonant or hard-sphere capture, whose magnitude is directly given by the dimensionless α reduced width amplitude $\theta_\alpha^{6.9}$ of the 6.9 MeV state which reflects the particle (α) properties of this state. Therefore a thorough measurement of the direct capture part of the cascade transition through the 6.9 MeV state could yield a precise determination of the α-width of this state. However, a more complete and self-consistent determination of the $E2$ ground state transition strength at low energies can be accomplished with the help of the proposed experiment by simultaneously measuring and fitting both the ground state and cascade transition data.

The connection between the cascade transition through the 6.9 MeV state and the d-wave properties of ^{16}O was noted in Refs. [7,9,15], where separate and simultaneous fits for the d-wave elastic phase shift, the cascade S-factor and the radiative ground state $E2$ transition were employed in different contexts. Ref. [15] indeed connects resonance R-matrix parameters and the direct capture process in a self consistent way. The cross section formulae from Ref. [15] relevant to the direct capture cascade cross section part are given in Sec. 6.2, Appendix 2.

In addition to the direct process, resonances in $^{12}C(\alpha,\gamma\gamma_{6.9})^{16}O$ will be present. States with $J^\pi=0^+$, 2^+, and 4^+ will interfere with the direct capture process in the total cross section, while resonances with different J^π will add incoherently. Resonances up to the proton threshold have been included in the following calculation; however, there is no radiative capture information available for the 3^- state at $E=4.42$ MeV and the 0^+ state at $E=4.89$ MeV [14]; in order to estimate their effects some γ-cascade strength has been assumed for these states. Existing cascade data [7,9] cover a range from E=1.4 MeV to 3.225 MeV where both of these states of unknown radiative decay strength are unimportant. The data include the 2.43 MeV 1^- resonance[5], the 2.68 MeV 2^+ resonance (though data are not published on top of it) and the 3.20 MeV 4^+ resonance [14]. The γ-strength for the 1^- and 4^+ state were fitted to the data (see discussion below); as in Ref. [9,15] it was assumed that the 7.1 MeV 1^- subthreshold state possesses negligible transition strength ($\gamma_\gamma^{7.1\rightarrow6.9}=0$) to the 6.9 MeV state; see, however, the discussion below. Other γ-strengths are taken from Ref. [14]; the lower 4^+ resonance has the largest cascade cross section because the 6.9 MeV cascade transition is the most likely γ-decay branch, while for the other resonances this branch is only of the order of a few percent. Boundary conditions were set on the subthreshold states for J=1 to 3 and at 3.20 MeV for J=4. For

---

[5]For an overview of resonances and state properties, see Sec. 6.3, Appendix 3.
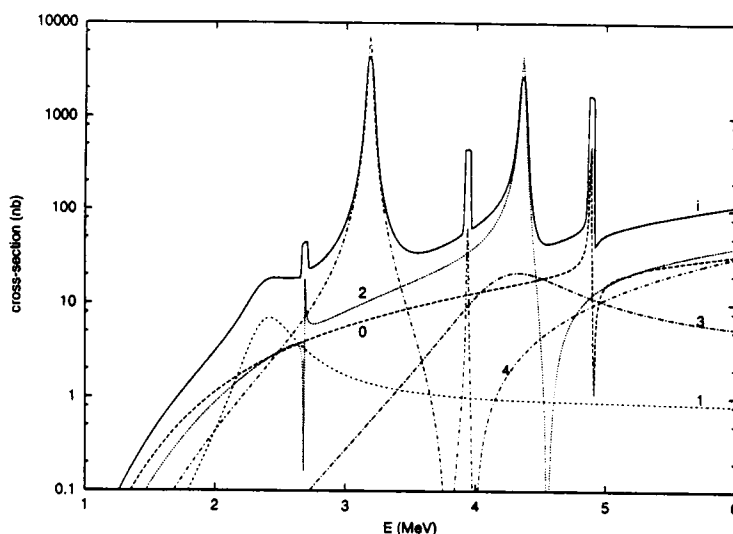
Fig. 3 R-matrix calculation of the cross section for the radiative capture into the 6.9 MeV state of ^{16}O. The decomposition into incoherent parts of the cross section is shown as indicated, as well as the summed cross section integrated over target thicknesses (straight line, labeled "i").

the fit to the data, integration over reasonable values of target thickness, beam energy spread and energy straggling was employed. In the calculations of the direct capture part, only $E2$ radiative transitions were assumed. This is, in principle, incomplete, as $2_i^+ \rightarrow 2_f^+$ transitions could also proceed via $M1$ radiation. However, in Ref. [16], the expected $M1$ matrix element is stated to be proportional to the magnetic moments of the particles in the transition, and thus are zero for pure α- and ^{12}C particles. Therefore a strong suppression of $M1$ (and other magnetic) isoscalar transitions is expected.

Figure 3 shows the expected total cross section as well as its decomposition into incoming partial waves ℓ_i=0...4. It is obvious from Fig. 3 that the direct capture in the E=1.5 to 6 MeV region leads to a distinguishable and measurable signal of approximately 0.3 to 100 nb. For the chosen resonance interference signs[6], the s-wave capture is then dominant at very low energies and significant in a region at about 5 MeV depending on the γ-strength of the 0^+ and 3^- resonances. The d-wave capture shows interferences with the two 2^+ resonances, but is about equally mixed between direct and resonance capture near 4 MeV and above 5 MeV. The g-wave capture is dominated by the 3.194 MeV 4^+ resonance, and shows a prominent interference pattern.

More information on the nature of the cascade-transitions can be gained by measuring the angular distribution of the primary γ-rays. Knowledge of the angular distribution is also desirable to make solid angle corrections for missing detector coverage. Relations for the angular distributions are given in Sec. 6.2, Appendix 2, showing the direct correlation between the partial wave cross sections. Note, that in these expressions for the angular distribution no 1^- and 3^- resonance strengths have been included. Indeed, the existence of any odd order Legendre polynomial in the angular distribution will tell about such

---

[6]The interference signs below 3.3 MeV were determined through least squares minimization to the data [7,9], while those above 3.3 MeV were arbitrarily selected.
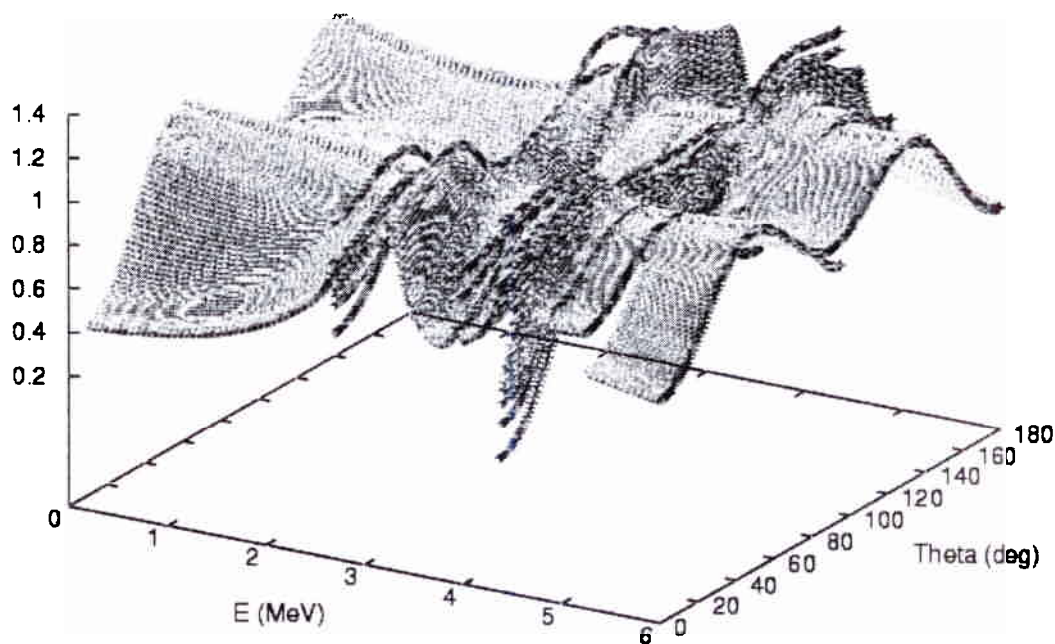
Fig. 4 Energy dependent angular distributions predicted for the E→6.9 MeV cascade transition.

admixtures. A measurement of the angular distribution of the primary γ-rays will provide the ratios of the partial wave cross sections independent of the fits to the total cross section, predicted distributions are shown in Fig. 4; the non-existence of odd Legendre polynomials shows as symmetry around $90°$.

If the $\ell=1$ pole strength of the subthreshold $E_x=7.1$ MeV state were measured independently (see below), the fit to the existing cascade data would likely provide excellent restrictions on $\gamma_{6.9}$. The best current fit to the cascade data [7,9] with $\gamma_\gamma^{7.1\to6.9}=0$ and $a=5.5$ fm is obtained for $\theta_\alpha^{6.9}=1.1\pm0.2$ ($\gamma_{6.9}=0.75\pm0.15$ MeV$^{1/2}$)^7 with a $\chi_\nu^2=0.90$ for the fit in good agreement with Ref. [15] ($\theta_\alpha^{6.9}=1.26$). In Ref. [7] a value of $(\theta_\alpha^{6.9})^2=1.0\pm0.2$ is quoted which would propagate to a similar error in $S_{E2}(300)$. In Ref. [9] values of $\theta_\alpha^{6.9}=0.66\pm0.07$ and $\theta_\alpha^{6.9}=0.53\pm0.05$, respectively, are derived depending on the value of $\gamma_\gamma^{7.1\to6.9}$, being zero for the first case. However, the mathematical approach used in Refs. [7,9] is different and not self consistent with R-matrix theory. Nevertheless, errors quoted are all reasonably small.

Figure 5 shows the present fit and data within their range and Fig. 6 shows the S-factor over an extended range with the data included.

The extrapolated cascade (6.9) S-factor at 300 keV is 7 keV b with errors omitted intentionally for this conditional fit. No radius dependence a on χ_ν^2 has been explored, because the cascade data pose little restriction on a by themselves [15]. In addition, any

---

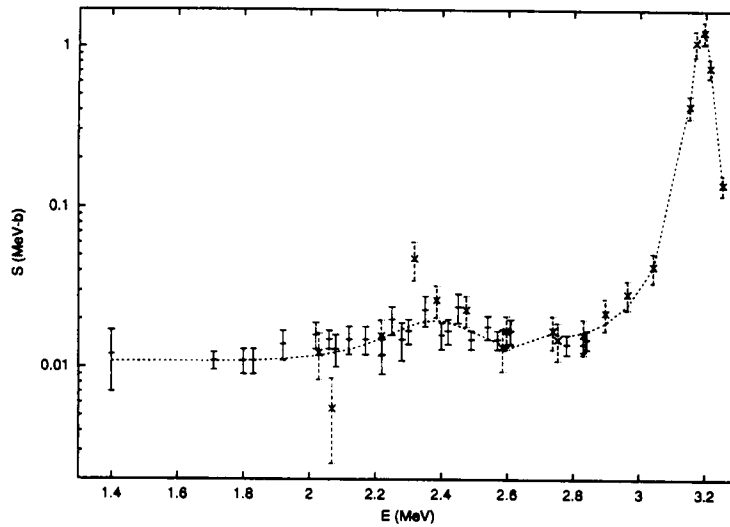[7]Errors derived as in Ref. [4] and comparable to those of $S_{E1}(300)$.

Fig. 5 R-matrix fit of the S-factor (dashed) to the radiative capture data of Ref. [7] (cross) and Ref. [9] (bar) into the 6.9 MeV state of ^{16}O.
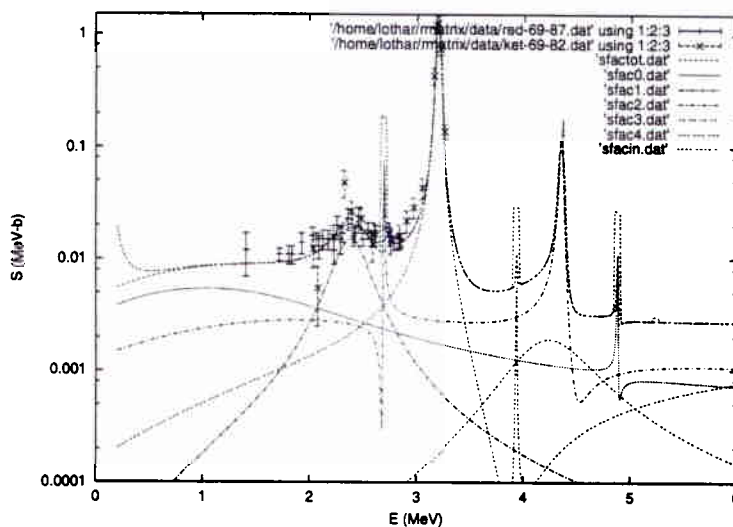

Fig. 6 R-matrix calculation of the S-factor (dashed) for the radiative capture into the 6.9 MeV state of ^{16}O. In addition, the decomposition into incoherent parts of the S-factor is shown as indicated, as well as an integration over target thicknesses (4 short dash-break line). The data of Ref. [7] (cross) and Ref. [9] (bar) are also shown.

finite γ-strength $\gamma_\gamma^{7.1 \to 6.9}$ will result in a larger error in the extrapolation of the cascade cross section to low energies than the a dependence; see below. In general, higher cascade S factors are expected for higher a [15]. Recent elastic scattering data [6], however, suggest tight limits on the interaction radius with $a=5.5$ fm is an acceptable value, see above. Therefore $S_{6.9}(300)=7$ keV b represents a lower limit for the 6.9 MeV cascade transition, which could be increased by additional $\ell=1$ strength.

The value of $\gamma_{6.9}=0.75\pm0.15$ MeV$^{1/2}$ for the best fit here is not in agreement with the analysis of Ref. [6], i.e. $\gamma_{12}=\gamma_{6.9}=0.47\pm0.06$ MeV$^{1/2}$ from elastic scattering; however the question of the unresolved $\ell=1$ subthreshold state remains for the cascade data. In Ref. [17] a value of $\gamma_{6.9}=0.33$ MeV$^{1/2}$ for $a=5.5$ fm was found. Lower values of $\gamma_{6.9}$ from the analysis of elastic phase shifts have been previously noted in Ref. [15] in similar fits to older scattering data [20] but using part of the cascade data employed here [9]. However, introducing a γ-strength $\gamma_\gamma^{7.1 \to 6.9}$ consistent with or lower than that of the $E_x=9.6$ MeV state for the $E_\gamma=0.2$ MeV 7.1 MeV$\to$6.9 MeV transition[8] and introducing background γ-strength leads to changes in the $\ell=1$ cascade cross section in such a way that the existing data can be quite well fitted over an extended range of values of $\theta_\alpha^{6.9}(\gamma_{6.9})$. This has also been indicated in Ref. [9]. If higher energy cascade data above 3.4 MeV were available, this uncertainty would be eliminated in the determination of $\theta_\alpha^{6.9}$, though not in the extrapolation of the cascade cross section itself. Therefore an independent measurement of the 7.1 MeV$\to$6.9 MeV transition in ^{16}O is strongly recommended (and will eventually been pursued), e.g. by a ^{19}F$(p,\alpha_4\gamma_{0.2}\gamma_{6.9})^{16}$O coincidence experiment. Such an experiment should strive for experimental limits of a few 10^{-6} in the 7.1 MeV$\to$6.9 MeV γ branching ratio.

It has been shown by now that the reduced α-width of the 6.9 MeV 2^+ state in ^{16}O can be uniquely determined (for a chosen channel radius a) by a measurement of the excitation function of the cascade transition through the 6.9 MeV state. In the all inclusive fit with experimental ground state data proposed here, the cross section part resulting solely from the dominant subthreshold pole [3] for the $E2$ ground state transition (ignoring small channel contributions) can then be written as

$$\sigma_{E2(0)} = \frac{10\pi}{k^2} P_2 \left| \frac{\frac{\gamma_{6.9}\Gamma_{\gamma 6.9}^{1/2}}{E_{6.9}-E}}{1-(S_2-B_2+iP_2)R_2} \right|^2 \tag{1}$$

where S_2, B_2, and R_2 are the shift, boundary and R-function in conventional notation [4], and $E_{6.9}=-0.245$ MeV(for the boundary condition determined at this energy). The relationship of the γ-width $\Gamma_{\gamma 6.9}$ of the 6.9 MeV state to the observed width is described in Ref. [4]. Therefore Eq. 21[9] relates the cross section for the cascade transition Eq. 17[9] to that for the ground state transition (Eq. 1) via $\gamma_{6.9}$. More extensive expressions including resonance states in the cascade direct capture, ground state direct capture, additional poles and channel effects on the γ reduced width amplitudes can be found in Ref. [15] and have been used in previous calculations [3,15].

It is therefore the magnitude of the cascade cross section which directly determines the reduced α-width of the 6.9 state. Knowledge of this width will put the extrapolation of the $E2$ ground state transition on a more solid footing and will hopefully reach agreement with

---

[8]Corresponding to a branching ratio 7.1$\to$6.9 of approximately 5×10^{-5} and lower.
[9]Sec. 6.2, Appendix 2

the elastic scattering data. This will reduce to a great extent this major uncertainty in the $^{12}C(\alpha,\gamma)^{16}O$ cross section at astrophysically important energies. It is therefore proposed that the excitation function of the 6.9 MeV cascade be measured with high statistical accuracy and systematic precision. The cross section calculations and literature presented here show that it is within experimental reach to obtain better than 10% precision for this width. In an additional experiment, the γ-strength of the $E1(M2)$ transition from the 7.1 to the 6.9 MeV state in ^{16}O should be determined which is particularly important for the interpretation of the low energy cascade data and their extrapolation to astrophysical energies in $^{12}C(\alpha,\gamma)^{16}O$. Because the ground state γ-transition in $^{12}C(\alpha,\gamma)^{16}O$ can be measured simultaneously with the 6.9 MeV cascade transition, it is suggested for this proposal that fits are performed to the ratios of differential and total cross sections. Such a method will eliminate or strongly reduce several experimental systematic uncertainties encountered in measuring absolute cross sections.

1.4.2   Other cascade transitions

The contribution of other cascade transitions to the $^{12}C(\alpha,\gamma)^{16}O$ cross section is thought to be small, however, they are badly known. In detail: for the 7.1 MeV 1^- state the 2.43 MeV resonance is visible. However, E1 direct capture from the s-wave is suppressed and the S-factor just drops off largely resonantly ($S_{7.1}(300) \approx$ 1-2 keV b [15]) with some E2 contributions from the p- and f-wave. Interestingly enough, the 7.1 MeV state can act in the 7.1 MeV cascade as subthreshold state as well. No resonance above 3 MeV is known to have a γ-branch into the 7.1 MeV state; therefore the direct capture cross section is expected to increase smoothly with energy at a low level compared to the 6.9 MeV branch.

The cascade transition to the 6.1 MeV 3^- state is likely weak due to the lack of resonances in the relevant region and the high angular momenta involved. The transition to the 6.0 0^+ state shows the same division into E1 and E2 transitions and the same angular momentum distribution as the ground state, but scaled by E_γ^3 or E_γ^5 dependences. It is thought to be weak, but data are scarce (only available in 2^+ resonances, see Sect 6.3, Appendix 3). The present proposal using γ-recoil and γ-γ recoil techniques will allow a thorough measurements of these cascade transitions.

1.5   New measurements of the ground state transition at high energies

The $^{12}C(\alpha,\gamma)^{16}O$ cross section needs to be extrapolated to a centre-of-mass energy of 300 keV and even below. Because this cross section cannot be deduced with the necessary precision from microscopic nuclear models (see, however, Sec. 1.6), it is necessary to rely on phenomenological descriptions of nuclear reactions, such as R-matrix theory for the extrapolation. Such an approach necessitates that a data set as large as possible be taken into account to limit as much as possible parameters in this theory like the α-strengths of subthreshold $^{12}C+\alpha$ states, the most important parameters in the problem. It is therefore proposed to extend the γ ground state decay measurement (simultaneously with the cascade measurements) to energies above 3 MeV in the center of mass (to 4.9 MeV, which is the ISACI limit) where no reliable data exist. This will allow to conclude directly on the ground state interference signs involved in the $^{12}C(\alpha,\gamma)^{16}O$ ground state
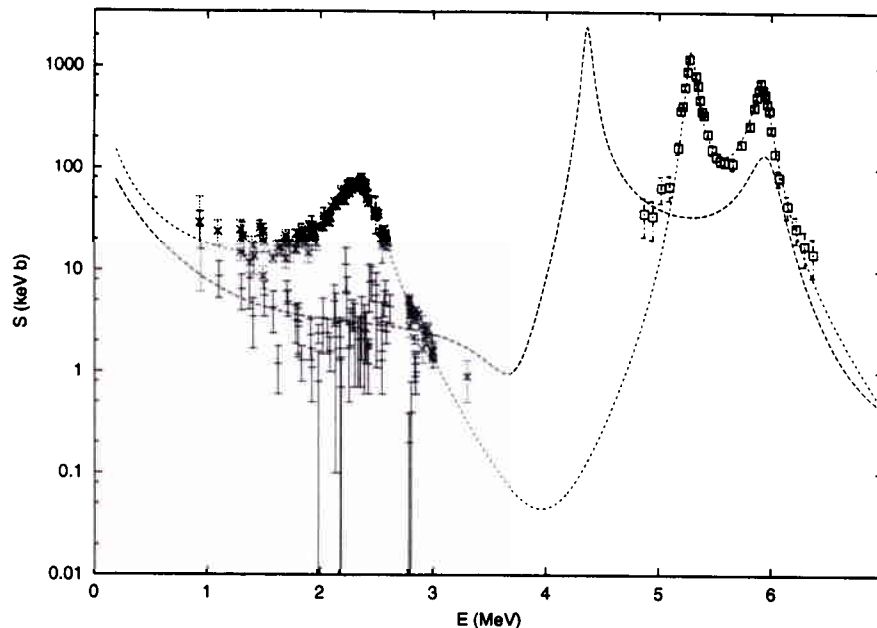
Fig. 7 Excitation curve of the ground state $E1$ and $E2$ transition S-factors in $^{12}C(\alpha,\gamma)^{16}O$ at a=5.5 fm. Some interference signs are arbitrarily chosen. Some data are included, in particular at high energies those (the only ones) of Ref. [18].

transition as well as put the direct component of the E2 transition at a better footing. The importance of determining the signs and shapes of these interferences have been both pointed out in Refs. [6] and [21] in particular those around the two 2^+ resonances in the energy region proposed to be measured. These also bear some direct correlations to $\gamma_{6.9}$ [21].

At TRIUMF we have a rich experience with the application of R-matrix theory and have developed a multitude of programs also coded in parallel program mode (MPI). In particular, higher energy data ([18] and references therein) can now be included in the fits. An example of such calculations for the ground state $E1$ and $E2$ transitions extended to higher energies is shown in Figure 7 as S-factor. The corresponding cross section is shown in Figure 8. An example for Monte Carlo simulations is shown in Fig. 9 using recent ($E1$) data measured in Bochum [19]. The Figure shows that with the data of Ref. [19] alone destructive and constructive interference between the subthreshold and the first above threshold 1^- state cannot be clearly distinguished [19] though all available data sets combined show a preference for a constructive interference in the low energy region [4]. However, both providing much improved low energy data, which is very difficult, as well as high energy data as planned here, will resolve the ambiguity.

It has been proposed that the E0 ground state transition (e^+e^- pair emission) may play a role in the $^{12}C(\alpha,\gamma)^{16}O$ total cross section. It would proceed as a direct process from the s-wave as there are no known 0^+ resonances in the region of interest. Theory predicts this transition to be small, but no data exist. A strong transition of this kind would show up as a difference between the γ tagged recoil data and the single recoil data after γ efficiency correction and thus demonstrates another advantage of doing $^{12}C(\alpha,\gamma)^{16}O$ with a recoil
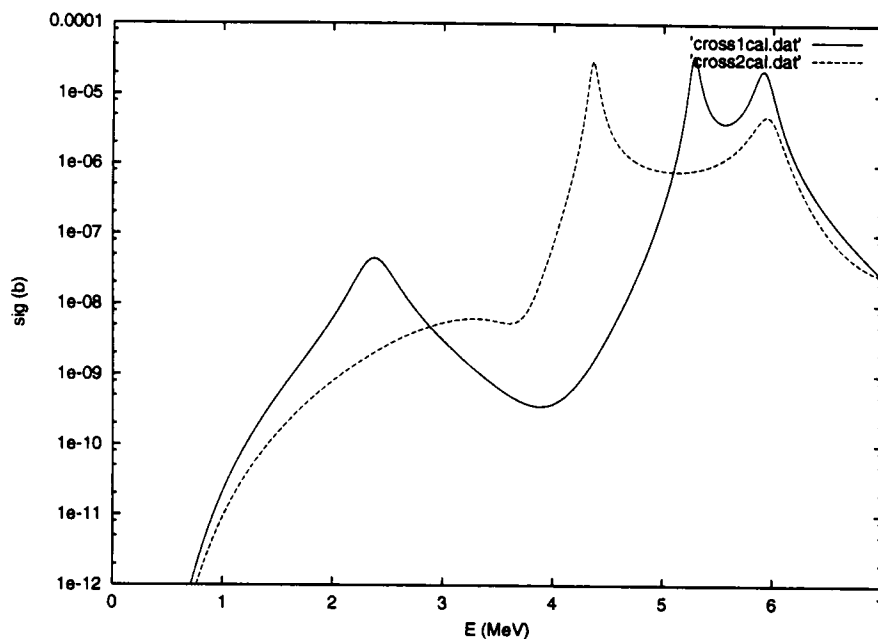
Fig. 8 Same calculations as for Fig. 7, but displaying cross sections.
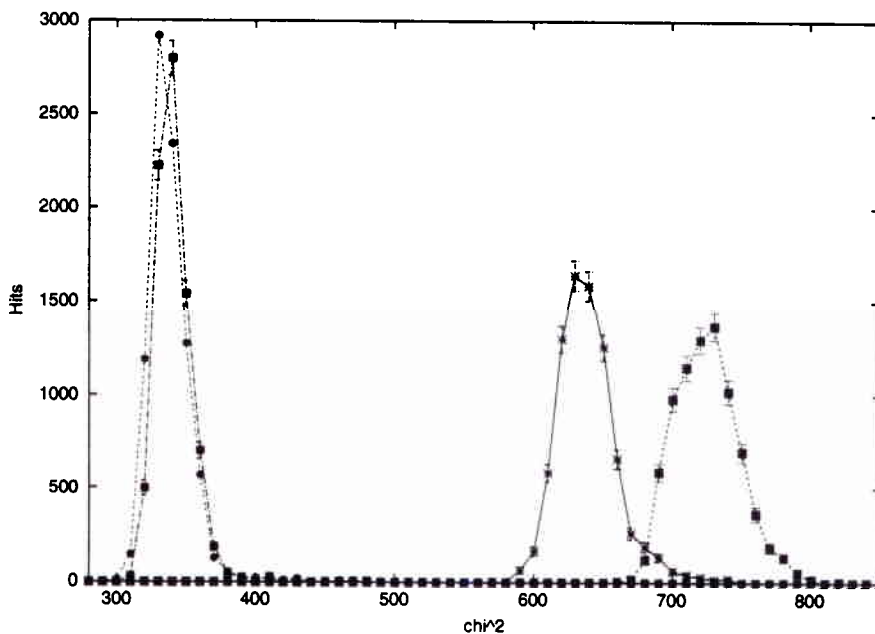
Fig. 9 Distribution of the least squares parameter χ^2 in a Monte Carlo simulation using different data sets: filled circle and square using data of Ref. [19] and [18] with forced destructive and constructive interference between the subthreshold and the first above threshold 1^- state, respectively; cross: same data and data of Ref. [19] extended to higher energies; open square: low energy data of Ref. [19] with half error, both forced on destructive interference for pseudo-data set with a constructive interference.

separator. Also tagging on the 511 keV e^+ decay line is possible, though the signal is not quite unique. If there is more evidence, direct e^+-e^- pair production can be observed with more sophisticated detectors, while the E_x=12.05 MeV 0^+ resonance may serve as a test ground.

Because all codes developed at TRIUMF fit experimental data it is imperative that they include correct treatment of experimental responses. These can only be included by experienced experimenters. Therefore a close collaboration between the people who do the fits and the experimenters is desirable. In the proposed experiment it is planned for probably the first time that both the analysis and data taking take place in mutual feedback.

1.6 Theoretical analyses of the elastic scattering and radiative capture data

In parallel with these experimental developments, we propose to compare different ways of analyzing both the elastic-scattering and radiative-capture experimental data. As explained above, a good fit of all the data can be obtained with the R-matrix phenomenological model. In particular, the elastic scattering data constrain the interaction radius a [6], which is the size of the square potential underlying the R-matrix theory. This fact suggests that the elastic scattering data could be used to construct a potential model, i.e. an interaction potential between the ^{12}C and α nuclei. This potential could then in turn be used to calculate radiative-capture cross sections. This would provide an interesting alternative to the R-matrix analysis and would give an estimate of the uncertainties due to the theoretical model in the low-energy extrapolation.

First attempts in this direction have been made in Ref. [20], using a less complete and less precise set of elastic-scattering data as the one presented in Subsec. 1.2. Accordingly, only simple form factors (Woods-Saxon or Gauss) were used and the data did not totally constrain the potential-model parameters. We believe the new set of data is sufficiently large to allow the use of more sophisticated techniques to construct interaction potentials, namely *inversion* methods [22]. The main advantage of these techniques is they do not require any assumption on the form factor of the potential: they rather *deduce* this form factor from the scattering data. In particular, an inversion method recently developed [25] has shown promising results for the $\alpha + \alpha$ interaction. This method, based on the algebraic formalism of supersymmetric quantum mechanics, allows either to fit scattering phase-shifts of different partial waves with the same local potential or to prove that such a potential does not exist. Answering this question for the $^{12}C + \alpha$ data is certainly important and in case a simple local potential can be found, it would constitute the simplest theoretical model ever constructed for this system. Moreover, the inversion technique of Ref. [25] makes use of rational expansion of partial waves S-matrices (as a function of the wave number). This constitutes an interesting alternative to R-matrix partial-wave parameterization; in particular, the values of the resonance energies and widths in both approaches could be compared.

A possible drawback of an approach based on pure elastic $^{12}C + \alpha$ data is the fact that the deduced potential may not carry adequate information on the internal structure of the two participant clusters, failing to give a proper description of internal structure of the composite 16-nucleon system. A complementary way of constructing interaction

potentials between nuclei is to deduce them from nuclear microscopic models (i.e. models that take all nucleons into account). As is well known, the positive energy part of the nucleon self-energy represents the correct microscopic realization of an optical model that fully describes the interaction with one more nucleon. The negative energy part can instead be used to generate the proper bound core + nucleon states, together with the relative overlap function. This approach, for the nucleus + nucleon case, has already been explored in the TRIUMF theory group by using one-body overlap functions. The method to construct the potential exploits the fact, that the one-body overlap functions are solutions of a Schrödinger-like equation [24]. Overlap functions, obtained by mean of shell-model [24] and self-consistent Green's function [26] calculations, have then been employed to extract a microscopic-based mean field potential. For instance, a satisfactory ^{16}O + nucleon potential has been constructed from a microscopic shell model of ^{17}F, by analyzing the states that have an ^{16}O + nucleon structure. It is tempting to generalize this method to nuclear states that have a core + cluster structure. For instance, a ^{12}C + α potential may be deduced from microscopic wave functions of ^{16}O states that have that structure; such wave functions could be for instance provided by the above mentioned many-body techniques or the microscopic cluster model [23]. By analyzing different states, the energy dependence of the potential could be studied and a comparison could be made with the inversion potential. Moreover, a comparison could be made between the capture cross sections calculated with the potential model and with the microscopic model from which it is deduced.

As regards of the Green's function approach mentioned above, a third possibility can be pursued. By following the approach of Ref. [27], a generalization of the nuclear self-energy to the case of the ^{12}C + α cluster structure can be achieved. Present calculations already give an adequate description of the 1^- and 3^- excited states of ^{16}O, which involve simple particle-hole configurations. In order to obtain a relevant description of the 0^+ and $2+$ levels, effects from two-cluster ^{12}C + α configurations have to be included. Finally it has been recently shown that resonant states close to the continuum receive non trivial contribution from unbound scattering states [28,29]. All these features appear to be relevant to the reaction that the present experiment aim to measure and can be properly included in a single calculation. Thus, the resulting 'cluster self-energy' would provide an (ab initio) exact microscopic tool to study the α capture reaction for both the scattering and resonant regimes, including α widths, as well as for the case of final bound states different from the ground state. In order to do this a preliminary inter-cluster potential, based on information from previous elastic scattering data measured [6], will also be helpful. In turn a complete description of the optical potential, that also include internal structure effects, will be achieved. We incidentally note that this last approach, although very sophisticated, is of high interests not only for the study of ^{12}C(α,γ) reaction but also because it would address several important nuclear structure issues, eventually leading to the most complete microscopical understanding of the nucleus ^{16}O.

2   Description of the Experiment

The reason, why α-capture data on ^{12}C are scarce above 3 MeV is increasing and overwhelming background from neutrons as the energy of the beam (either α or ^{12}C) increases. With the use of a recoil separator this background will be entirely removed,
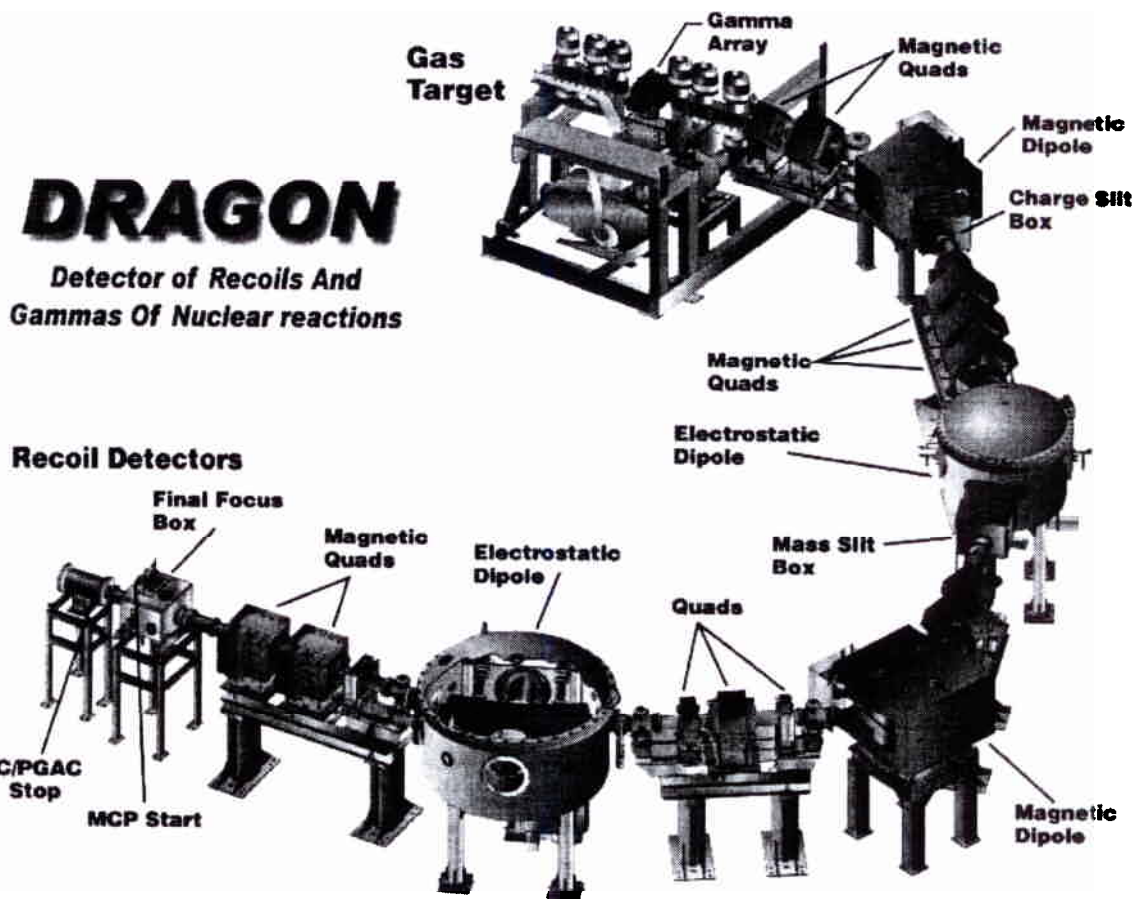
Fig. 10 Overview of the DRAGON recoil separator.

because the heavy ion detection is far away from the neutron production and not very sensitive to neutron detection at all. In addition, the time of flight condition for γ-particle recoil coincidences through DRAGON of the order of 2 μs reduces random coincidences and room background considerably. Furthermore, gating on the RF structure of the beam, will allow to suppress γ-events from background neutron capture. Therefore the recoil spectrometer DRAGON has the opportunity to open up a new era in the measurement of $^{12}C(\alpha,\gamma)^{16}O$. The recoil separator DRAGON is shown in Fig. 10; a description can be found in Ref. [30].

2.1 ^{12}C beam intensity

There is, however, one clear limitation on the existing ISAC RFQ-DTL system which must be overcome: At present after the RFQ, a carbon foil stripper increases the typical 1^+ charge state of the low energy heavy ion to a charge to mass ratio of better or equal 1/6 which is the acceleration limit of the DTL. This limits the heavy ion current to typically 1 particle (p)nA due to foil survival times. For $^{12}C(\alpha,\gamma)^{16}O$ measurements this is not competitive. It is proposed here that TRIUMF commits to the minimal effort of increasing this current to 1 pμA and more. This is in principle possible in two ways:

either by the installation of a gas stripper after the RFQ or extracting a doubly charged ^{12}C beam from OLIS or elsewhere with sufficient intensity. As a minimum requirement for the feasibility of the experiment, we request therefore that the production of multiple charged ^{12}C ions be thoroughly investigated at OLIS and, if necessary, a gas stripper (interchangeable with the foil one) be installed at the present stripper position. When the charge breeder is installed (2004?) it may also act as a source of multiply charged light ions, which is an option to be seriously tested. A 1 pμA beam limits the cross section measurements doable with good statistics in a reasonable time to about 1 nb. A recent preliminary measurement at OLIS shows that about 20 to 100 pnA of ^{12}C^{2+} and 12 pμA of ^{12}C^{+} can be produced. The ^{12}C^{2+} current which can already be produced is sufficient to start initial experiments.

2.2 Basic kinematics and modifications to DRAGON

When the γ-ray is emitted it puts momentum on the recoil particle resulting in an increased transverse and longitudinal phasespace of the recoil particle. The maximum recoil angle and energy gain can be calculated and are shown in Fig. 11. DRAGON has been designed to accept an angular recoil spread of 20 mrad, and a $\pm$4% variation in recoil energy. As can be seen from Fig. 11 this condition is well met for energies above 2.75 MeV. The opening angle of the exit restrictive tubes of the gas target are built for the 20 mrad acceptance. These need to be opened up slightly to allow for complete measurements down to 2 MeV. Since we are running with helium gas, the increased pressure loss should not cause a problem.

At the recoil angle imposed by ^{12}C(α,γ)^{16}O we cannot expect full transmission with the present DRAGON system at the lowest energies below 2.75 MeV, though we still may find a tune to do so. To ensure a larger acceptance of DRAGON we have performed beamtransport calculations with a quadrupole doublet at 50 cm away from the target centre position. This is roughly at the second pumping stage of the gas target. With such quadrupoles the acceptance angle can be boosted to about 35 mrad without recoil losses occurring. The pole tip field of such a quadrupole magnet has to be of the order of 2 kG which can be achieved by permanent SmCo magnets. Acceptance tests as described below will, however, be performed to test the true performance of DRAGON (Sec. 3).

2.3 Angular distributions

Angular distributions can be measured both with the recoil detector and the BGO (γ-detection)-array.

2.3.1 Recoil distribution

For the recoil detection the γ-emission angle translates into an energy change of the recoil particle via

$$E_r = \frac{m_b}{m_r} E_b + \frac{E_\gamma^2}{2 m_r c^2} - E_\gamma \sqrt{\frac{2 m_b E_b}{m_r^2 c^2}} \cos \theta_\gamma \tag{2}$$
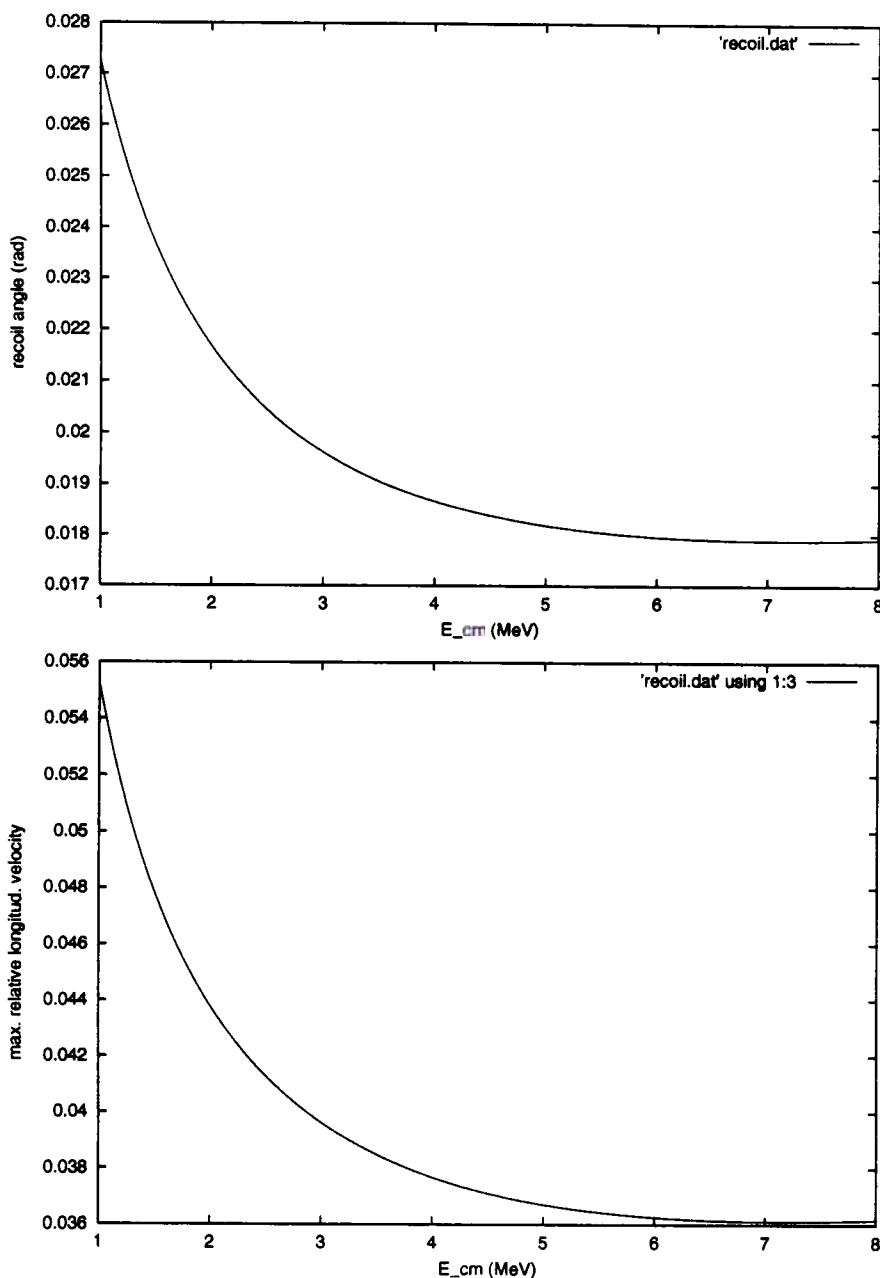
Fig. 11 Upper panel: maximum recoil opening angle vs centre-of mass energy for $^{12}C(\alpha,\gamma)^{16}O$. Lower panel: maximum relative energy change vs centre-of mass energy for $^{12}C(\alpha,\gamma)^{16}O$.

with r indicating recoil properties, m_b the beam particle mass, and E_γ the γ energy of the γ-ray emitted under an angle θ_γ.

Employing Eqs. 5 and 2 (Sec 6.1, Appendix1) the expected energetic distribution of the recoil ^{16}O can be calculated and is shown in Fig. 12 for three energies. These distributions have to be folded with the energy resolution of the silicon detectors which is less or equal 1% which is quite negligible in Fig. 12.

The recoil distribution (Fig. 12) is for γ-ungated events of the ground state decay. If a coincidence with one or more γ-detectors is requested, a cut will be imposed on the recoil spectrum. Our first tests will be designed, to measure precisely what γ and recoil angular distributions and their respective resolutions we will have to expect. For cascade transitions the single recoil distribution will be smeared, due to the fact that two γ-rays are emitted in generally different directions. Gating with the γ array will be required. The fraction of cascade events in the single spectrum has to be estimated from the coincidence spectra. However, it is expected to be small except for the 4^+ resonances along the excitation function which will serve as a test. As a matter of fact, the cascade fraction may be marginally enhanced in the single spectra at the extreme energies (angles), as the γ-rays from ground state emission do not have events at 0° and 180°. For recoil particle detectors we propose to use the present DSSD (Double Sided Strip Detector) as silicon detectors have been shown to have the best possible energy resolution.

In the past, a minuscule fraction of the beam has been detected at the final heavy ion detector ("leaky beam"); for a hydrogen target these events came always at the beam energy position energetically higher than the recoil events. In one run with a helium target using a resonance of ^{14}N$(\alpha,\gamma)^{18}$F at 382 keV/u, beam induced events were, however, observed below the recoil events. From this resonance the beam suppression can be deduced and has been found to be of the order of 10^{-15} for BGO (Bismuth Germanate)-recoil coincidences. However, the leaky beam always showed a strong energy dependence and the run was not fully optimized for beam transmission and slit setting. If leaky beam, what yet has to be tested proves to be detrimental, the ion chamber can be used which for the energies proposed will have a clear separation of ^{12}C and ^{16}O, or a local time-of-flight device with two MCPs (Multi Channel Plate), one of them would be still to be built.

2.3.2 γ-angular distribution and detection issues

The γ detection array will consist (subject to tests) of the present BGO detectors with two high volume germanium detectors at the centre close to the gas cell. For the gas cell the present design is sufficient. The reason why germanium detectors are needed is that the primary and secondary lines from cascade decays through the 6.9 MeV and the 7.1 MeV states are only separated by 200 keV which cannot be sufficiently resolved by the BGO detectors. However, even without a separation of the 6.9 MeV and the 7.1 MeV state, the different energy dependence of the cross section and the angular recoil distributions will likely allow a reasonable separation in fits to the data.

One major consideration with the use of Germanium detectors is the broadening of the γ-lines by the Doppler effect. It is

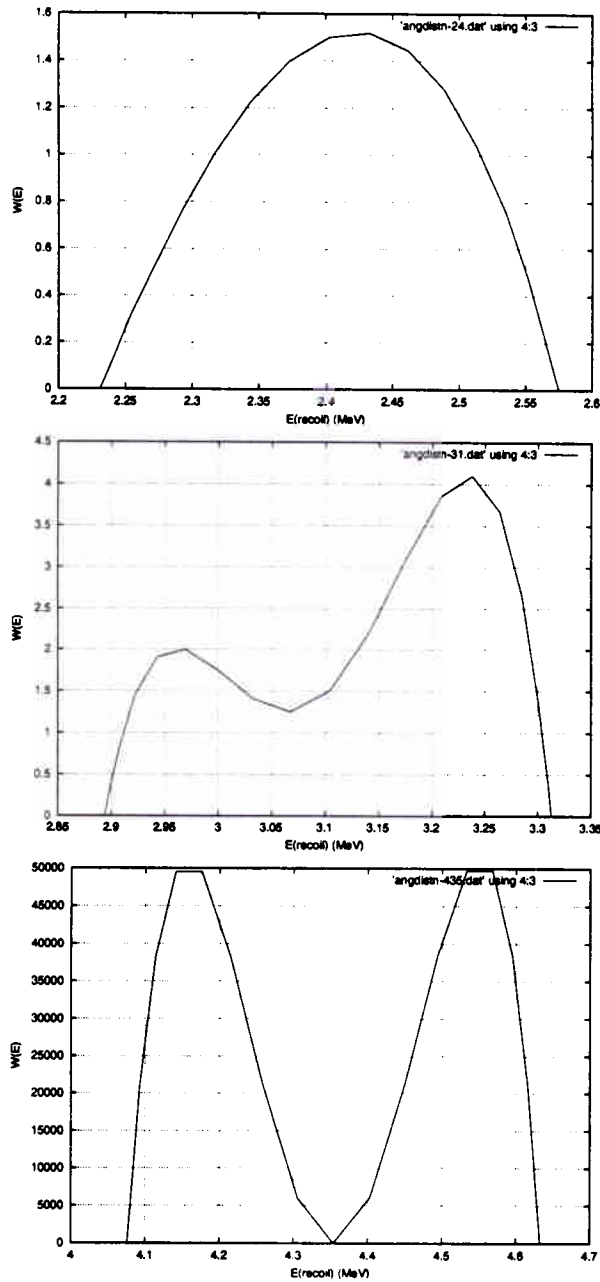$$E' = E \frac{\sqrt{1 - \beta^2}}{1 + \beta \cos \phi'} \tag{3}$$

Fig. 12 Energetic distribution of the recoil ^{16}O for three energies (2.4, 3.1, and 4.35 MeV) where (2.4 MeV) the 1^- part is dominant, the 1^- and 2^+ parts are about equal (3.1 MeV), and (4.35 MeV) the 2^+ part is dominant.

with $\beta = v/c$ and ϕ' the observing angle. This restricts the angular acceptance of a 5 cm germanium detector to 18° (for a 1 MeV/u ^{12}C beam) for 100 keV spread. However, we expect a better positional resolution from the clover detector. With 5 cm extension, the detector would have to be positioned 15 cm away from the target cell, where the BGO detectors would serve as an active shield. The present TIGRESS design calls for 3 cm resolution initially proposed to improve to 5 mm by electronic means till 2008. However, we will use the Notre Dame clover detectors which have a few cm intrinsic resolution. The time structure of the beam should provide for some left-right discrimination of the γ-rays. However, even if the two decay lines overlap in the germanium spectrum, the intrinsic resolution of the germanium detector of a few keV will allow to place cuts at different points of the spectrum and allow to fit different portions out of it as well as to select recoil particles with different ratios of 6.9 and 7.1 MeV contributions. In particular, extremes of the spectrum will only contain contributions from one transition.

2.4 Beam energy calibration and other DRAGON issues

At the moment, there is an ongoing effort to calibrate the ISAC-DTL beam via two magnets (Prague magnet after the DTL and DRAGON-MD1). This effort is soon to be completed. In addition, the ^{12}C(α,γ)^{16}O reaction is more or less self calibrating as all resonances are known to better than 1 keV precision. For the highest energy and a 4$^+$ charge state of ^{16}O, the voltage on ED1 has been calculated to be 185 kV, which is high, but still feasible. The voltage on ED2 is about 20% less. However, a 4$^+$ ^{16}O charge state in experimental running (except for tests) is not likely to be used as the charge-to-mass ratio is identical to ^{12}C^{3+}. Indeed, one would run a charge state of 5$^+$ for the higher energies.

For beam current normalization, periodic readings of the Faraday cups will be taken, while the relative intensity will be monitored by elastic scattering. An additional current reading can be obtained at the mass slit position.

It is planned to check charge state distributions periodically at different energies, by switching between different charge states of the recoiling ^{16}O and also comparing charge state distributions to an ^{16}O beam directly.

It is conceivable that a small parasitic beam of ^{16}O is part of the ^{12}C beam having the same energy as the ^{16}O formed in the ^{12}C(α,γ)^{16}O reaction. The effect is highly unlikely as the linear accelerator acts as a velocity filter. The parasitic ^{16}O contribution can be easily tested by removing the target gas and tuning DRAGON for recoils. Such an effect should be, in addition, totally suppressed by γ coincidences. In the unlikely case that there is a real problem, the installation of a Wien filter in front of DRAGON would remove such a beam.

3 Readiness

DRAGON is ready for initial tests in which we will scan the 1$^-$, 2$^+$, 4$^+$ and 2$^+$, resonances where angular distributions, branching ratios and cross sections are known. Those are at 0.81, 0.89, 1.065, 1.31 and 1.45 MeV/u (Sec. 6.3, Appendix3). In addition,

some exploratory runs will be done on the 3^- and 0^+ resonances with the latter at about the maximum energy of the ISAC-DTL. At the energy of the 4^+ resonance the 6.9 MeV cascade transition will be particularly strong, at the 1^- and 2^+ resonances the ground state transition will lead to the respective characteristic angular distributions. The 2^+ resonances also show strong decays in the 6.0 MeV state of ^{16}O. In all cases, the acceptance of DRAGON can be thoroughly tested and compared to beam transport calculations. In addition, scans of resonances will allow to determine target properties and reproducibility items. Test runs on the narrow 0^+ resonance and the wide 3^- resonance may result in radiative decay schemes which are by themselves publishable.

These tests will provide input to possible modifications of DRAGON, which may involve some mechanical reconstruction of the downstream part of the gas target, in which case funds will be sought from NSERC. In addition, the optimal γ-detector configuration will be explored. These modifications are expected to be ready in the second year by which time also the gas stripper should be installed after the RFQ and the germaniums be in place. After that full data taking can commence.

4 Beam Time required

The relation for an extended gas target between the target pressure p, its effective length l and the areal number of atoms is

$$F = 3.52 \times 10^{16} p[\text{T}] \, l \, [\text{cm}] \, [\frac{\text{atoms}}{\text{cm}^2}] \, . \tag{4}$$

We are confident to be able to run pressures up to 10 T in the extended gas target, thus with a measured l=10 cm, F=3.5$\times 10^{18}\text{cm}^{-2}$. Therefore with a 1$\mu$A beam 76 events/hour are expected into 4π. With a conservative γ detection efficiency of 30% (BGO and charge state) this leads to 23 events/hour. Typically a few hundred events would be aimed for, roughly the yield of 1 day. However, at most energies, cross sections are far higher. Typical run times there would be of the order of 1 hour or less. The coincidence γ-recoil efficiency with a clover detector will be likely lower, i.e. about 5%. This still allows measurements down to a few nb; however the cascade 6.9 transition generally has more than 10 nb cross section, see Fig. 3. With the gas stripper, in addition, more beam current (10 pμA) should be available.

The typical energy loss of the beam in the target (1 MeV/u) will be 15 keV in the centre-of mass, i.e., the target is relatively thin, except for the few narrow resonances. We propose to cover the energy region (2-4.9 MeV (cm)) in approximately 100 keV steps (cm), i.e. about 30 steps. However in resonance regions the stepwidth will have to be chosen smaller, on the other hand, cross sections are high. Prior to that, we have to test acceptance, efficiency, and angular distribution issues, which will be largely performed on resonances. We request 30 shifts for these tests and will report back to the EEC, as well as likely compose an NSERC grant application in October 2003.

We have found at DRAGON that a major fraction of our beamtime is spent on doing energy changes, taking 1 to 10 hours in time with sometimes little correlation to the magnitude of the step. In particular on resonances, the total experimental time needed is largely all spent on accelerator tuning. We therefore request about a 100 shifts of STABLE

beam time to do the final experiment, but will report back to the EEC far before this limit has been reached.

It should be pointed out that the split in radioactive beam time between the low energy area and the high energy area is about 2/3 to 1/3 at moment, and certainly the use of the low energy area will stay high. In addition, there are extended cyclotron maintenance periods. This leaves plenty of time for stable beam operation at DRAGON. In addition, the development of new radioactive beams is very slowly progressing. DRAGON has so far received one radioactive species, and for 2003, may receive another one. On the other hand, DRAGON is a three million dollar facility and should not be left to idling when it can be used in a very important experiment.

5 Data Analysis

In general, the data amount produced at DRAGON is small (100 MB per run or so) and can be rather quickly analyzed. This data amount may drastically increase, if and when time digitized information from the clover detectors will become available. Basically results will appear on-line after all cuts have been figured out in the tests. However, we plan to do rather immediate theoretical fits on our results, which are far more involved, but with whom we have a great amount of experience. They usually require extensive computing. Actual measurements performed will be driven by these fits. We expect that the computing can be done with facilities available for TUDA analysis and the use of WESTGRID[10].

---

[10]High power computing network in Western Canada.

6 Appendices

6.1 Appendix 1: Relations for the ground state transition

If each ground state decay mode (E1 or E2) in $^{12}C(\alpha,\gamma)^{16}O$ were the only one taking place, it would produce quite distinct angular pattern in the decay, i.e. a dipole pattern ("handle") and a quadrupole pattern ("butterfly"). Where the respective strength of both transitions is comparable the angular radiative distribution for the ground state is an interference pattern between the two extremes, i.e.

$$W(\theta_\gamma, E) = \quad 1 - Q_2 P_2(\cos\theta_\gamma) + [\sigma_{E2}(E)/\sigma_{E1}(E)] \quad \times [1 + \frac{5}{7}Q_2 P_2(\cos\theta_\gamma) - \frac{12}{7}Q_4 P_4(\cos\theta_\gamma)]$$
$$+ \frac{6}{5}[5[\sigma_{E2}(E)/\sigma_{E1}(E)]]^{1/2} \cos\Phi(E) \quad \times [Q_1 P_1(\cos\theta_\gamma) - Q_3 P_3(\cos\theta_\gamma)] \,, \quad (5)$$

where $P_k(\cos\theta_\gamma)$ are the Legendre polynomials, Q_k are the experimental attenuation coefficients of the γ detectors and $\Phi(E)$ is the phase difference between the d and p wave and a Coulomb phase given as

$$\Phi(E) = \delta_2(E) - \delta_1(E) + \arctan\frac{1}{2}\eta \quad (6)$$

with η being the Sommerfeld parameter. Therefore a fit to a radiative angular distribution in $^{12}C(\alpha,\gamma)^{16}O$ is largely sensitive to the ratio of the E1 and E2 cross sections as phaseshifts are known from elsewhere.

The E1 data are fitted with[11]

$$\sigma_{E1}^0(E) = \frac{6\pi}{k^2} P_1(E) \left| \frac{\sum_\lambda \frac{\gamma_\lambda \Gamma_{\lambda\gamma}^{1/2}}{E_\lambda - E}}{1 - (S_1(E) - B_1 + iP_1(E))R_1(E)} \right|^2 \quad (7)$$

and the energy dependent γ-width

$$\Gamma_{\lambda\gamma} = 2E_\gamma^3 \gamma_{\lambda\gamma}^2 \quad (8)$$

for the radiative capture and

$$W(E) = f_\beta(E) \sum_{\ell=1,3} P_\ell(E) \left| \frac{\sum_\lambda \frac{A_{\lambda\ell}}{E_{\lambda\ell} - E}}{1 - [S_\ell(E) - B_\ell + iP_\ell(E)]R_\ell} \right|^2 \quad (9)$$

for the ^{16}N β-delayed α-spectrum. Here the index λ indicates summation over states, The index 1 indicating an angular moment of 1, the index γ indicates that the symbol refers to radiative properties. $P(E)$ with an energy indicator refers to the penetrability, $S(E)$ are the shift functions and B the boundary conditions. The R-function is given by

$$R_\ell(E) = \sum_\lambda \frac{\gamma_{\lambda\ell}}{E_{\lambda\ell} - E} \,. \quad (10)$$

For the ground state E2 transition in $^{12}C(\alpha,\gamma)^{16}O$ is

$$\sigma_{E2}^0 = \frac{5\pi}{k^2} |U_0^2(E)|^2 \quad (11)$$

---

[11] Due to the effective mass, see below, the external parts of the cross section are suppressed.

with the scattering function

$$U_0^2(E) = -ie^{i\Omega_2} 2P_2^{1/2} k_\gamma^{5/2} \left[\sum_{\lambda\mu} \gamma_\lambda^2 \gamma_{\mu\gamma 0}^2 A_{\lambda\mu}^2 + \frac{3}{\sqrt{10}} \frac{M_n^{1/2} e}{\hbar k} N_f^{1/2} a^2 F_2(a) G_2(a) \theta_\alpha^0 (2200|00) J_2'(2,0)(E) \right]$$

(12)

with $A_{\lambda\mu}$ being the elements of the state matrix [15] (for more notations see Eq. 18). $\Omega_2 = \omega_2 - \phi_2$, ω_2 is the Coulomb phase shift, ϕ_2 the hard sphere phase shift [15], P_{ℓ_i} the penetrability, $k_\gamma = \frac{E_\gamma}{\hbar c}$ the radiative wave number, M_n the atomic mass unit, e_q the electric unit charge, and $F_{\ell_i}(a)$ and $G_{\ell_i}(a)$ the regular and irregular Coulomb functions at the radius a, respectively. Therein is M_n the atomic mass unit (931 MeV/c^2). From the normalization of the wave functions comes

$$N_f^{-1} = 1 + \frac{2(\theta^0)^2}{a} \int_a^\infty dr \left[\frac{W_0(r)}{W_0(a)} \right]^2$$

(13)

with the dimensionless reduced width amplitude for the α-particle

$$\theta_\alpha^0 = \gamma^0 (\hbar^2/\mu a)^{-1/2} .$$

(14)

$W_J(r)$ are the Whittaker functions, i.e. to a very good approximation the continuation of the bound state wavefunction outside the channel radius a. In similar fashion is

$$J_2'(2,0)(E) = \frac{1}{a^3} \int_a^\infty dr \, r^2 \frac{W_0(r)}{W_0(a)} \left[\frac{F_2(r)}{F_2(a)} - \frac{G_2(r)}{G_2(a)} \right] .$$

(15)

Note the overlap between the Whittaker ground state function (index 0) and the Coulomb scatter functions (index 2) in this integral $J_2'(2,0)$.

The γ-width $\gamma_{\mu\gamma 0}^2$ can in principle be divided into an internal and external region

$$\gamma_{\mu\gamma 0}^2 = \gamma_{\mu\gamma 0}^2(\text{int}) + \gamma_{\mu\gamma 0}^2(\text{chan})$$

(16)

with the internal part normally dominant and the channel part given by a similar expression (Eq. 12, [15]) as the direct one.

6.2 Appendix 2: Relations for the 6.9 MeV cascade transitions

As in Ref. [15] the hard-sphere (external part of the transition) cross section is ($\ell_f = 2$)

$$\sigma_{DC \to 6.9}(E) = \frac{\pi}{k^2} \sum_{\ell_i = 0,2,4} (2\ell_i + 1)|U_{6.9}^{\ell_i}(E)|^2$$

(17)

where k is the α-particle wave number and the scattering function is

$$U_{6.9}^{\ell_i}(E) = \frac{-6i}{\sqrt{10}} \frac{M_n^{1/2} e_q}{\hbar k} e^{i(\omega_{\ell_i} - \phi_{\ell_i})} P_{\ell_i}^{1/2} k_\gamma^{5/2} N_f^{1/2} a^2 F_{\ell_i}(a) G_{\ell_i}(a) i^{\ell_i} \theta_\alpha^{6.9} (\ell_i 200|20) J_2'(\ell_i, 2).$$

(18)

The summation extends over the three possible incoming angular momenta for $E2$ capture into the 6.9 MeV state, i.e. s-, d-, and g-wave (similar to Eq. 13) Both N_f and $J_2'(\ell_i, 2)(E)$

which stem from the overlap between the wave function of the bound ground state and the external Coulomb functions are (similar to Eqs. 13 and 15) as

$$N_f^{-1} = 1 + \frac{2(\theta_\alpha^{6.9})^2}{a} \int_a^\infty dr \left[\frac{W_2(r)}{W_2(a)}\right]^2 \tag{19}$$

and (see Eq. 15)

$$J_2'(\ell_i, 2)(E) = \frac{1}{a^3} \int_a^\infty r^2 dr \frac{W_2(r)}{W_2(a)} \left[\frac{F_{\ell_i}(r)}{F_{\ell_i}(a)} - \frac{G_{\ell_i}(r)}{G_{\ell_i}(a)}\right] . \tag{20}$$

Note that $\theta^{6.9}$ is common to the three incoming partial waves in the summations of Eqs. 17. The reduced width amplitude in this case (Eq. 14) $\gamma_{6.9}$ (aka γ_{12}) is related to the dimensionless reduced width[12] via

$$\theta_\alpha^{6.9} = \gamma_{6.9}(\hbar^2/\mu a^2)^{-1/2} \tag{21}$$

with the reduced mass μ of the ^{12}C$+\alpha$ system.

Following Ref. [31] the angular distributions for the individual partial waves (s, d, g) are

$$
\begin{aligned}
W_0(\theta) &= 1 & (22) \\
W_2(\theta) &= 1 - 0.1531 P_2(\cos\theta) - 0.4898 P_4(\cos\theta) & (23) \\
W_4(\theta) &= 1 + 0.5102 P_2(\cos\theta) - 0.3745 P_4(\cos\theta) . & (24)
\end{aligned}
$$

These mix coherently (though not the s and g wave), resulting in an angular distribution expressed as $W(\theta) = \sum a_k P_k(\cos\theta)$ with

$$a_0 = 1 \tag{25}$$

$$a_2 = \frac{1}{1 + y_{02} + y_{24}} [-0.1531 y_{02} + 0.5102 y_{24} - 1.1952\sqrt{y_{02}}\cos\epsilon_{02} - 0.5476\sqrt{y_{24}}\cos\epsilon_{24}] \tag{26}$$

$$a_4 = \frac{1}{1 + y_{02} + y_{24}} [-0.4898 y_{02} + 0.375 y_{24} + 1.82538\sqrt{y_{24}}\cos\epsilon_{24}] , \tag{27}$$

where $y_{02} = \frac{\sigma_2}{\sigma_0}$ and $y_{24} = \frac{\sigma_4}{\sigma_2}$ are the ratios of the total cross sections for the respective partial waves, respectively; and the phases $\epsilon_{\ell_i \ell_i'}$ are

$$\epsilon_{\ell_i \ell_i'} = \omega_{\ell_i'} + \delta_{\ell_i'} - \omega_{\ell_i} - \delta_{\ell_i} \tag{28}$$

where ω_{ℓ_i} is the Coulomb phase of partial wave ell_i and δ_{ℓ_i} its nuclear phase.

6.3   Appendix 3: Resonance properties relevant to ^{12}C$+\alpha$

Properties of resonant states are listed in Table 1 as compiled from different sources [6,14].

---

[12]Note that in Ref. [15], for historical reasons, two dimensionless reduced widths, θ_α and θ_f, are used and distinguished by a factor $\sqrt{3/2}$.

E_x (MeV)	E (MeV)	Γ (keV)	E_{lab}/u (MeV/u)	J^π	E_f (MeV)	Branch (%)
9.59	2.43	400±20	0.81	1^-	0	63±6
					6.92	6±6
					7.12	31±6
9.84	2.68	0.6±0.1	0.89	2^+	0	61±4
					6.05	18±4
					6.92	21±4
10.36	3.20	26±3	1.07	4^+	6.92	100
11.10	3.94	0.28±0.05	1.31	4^+	6.13	55±23
					6.92	45±11
11.52	4.36	71±3	1.45	2^+	0	91.7
					6.05	4.2±0.7
					6.92	4.0±1.0
					7.12	≤0.8
11.58	4.42	855±15	1.47	3^-		
12.05	4.89	1.5±0.5	1.63	0^+	0	a

^{a} Monopole element known from electron scattering.

Table 1 Resonances and γ-decay properties in $^{12}C+\alpha$.

References

1. S.E. Woosley, A. Heger, T. Rauscher, and R.D. Hoffman, proceedings of Nuclei in the Cosmos VII, Nucl. Phys., to be published.

2. T.A. Weaver and S.E. Woosley, Phys. Reports, **227**, 65-93 (1993).

3. L. Buchmann, R.E. Azuma, C.A. Barnes, J. Humblet, and K. Langanke, Phys. Rev. C, **54**, 354 (1996).

4. R.E. Azuma, L. Buchmann, F.C. Barker, C.A. Barnes, J.M.D'Auria, M. Dombsky, U. Giesen, K.P. Jackson, J.D. King, R.G. Korteling, P. McNeely, J. Powell, G. Roy, J. Vincent, T.R. Wang, S.S.M. Wong, and P.R. Wrean, *Phys. Rev. C*, **50**, 1194 (1994).

5. S. Woosley, UCSC, private communication, 2000

6. P. Tischhauser, R.E. Azuma, L.Buchmann, R. Detwiller, U. Giesen, J. Görres, M. Heil, J. Hinnefeld, F. Käppeler, J.J. Kolata, H. Schatz, A. Shotter, E. Stech, S. Vouzoukas, and M. Wiescher, Phys. Rev. Lett, **88** 072501 (2002).

7. K.U. Kettner, H.W. Becker, L. Buchmann, J. Görres, H.Kräwinkel, C. Rolfs, P. Schmalbrock, H.P. Trautvetter, and A.Vlieks, Z. Phys. A, **308** 73 (1982).

8. P. Dyer, C.A. Barnes, Nucl. Phys. A, **233**, 495 (1974).

9. A. Redder, H.W. Becker, C. Rolfs, H.P. Trautvetter, T.R. Donoghue, T.C. Rinkel, J.W. Hammer, and K. Langanke, *Nucl. Phys. A*, **462**, 385 (1987).

10. R.M. Kremer, C.A. Barnes, K.H. Chang, H.C. Evans, B.W. Filippone, K.H. Hahn, and L.W. Mitchell, Phys. Rev. Lett. **60**, 1475 (1988).

11. J.M.L. Ouellet, N. Butler, H.C. Evans, H.W. Lee, J.R. Leslie, J.D. MacArthur, W. McLatchie, H.-B. Mak, P. Skensved, J.L. Whitton, and X. Zhao, Phys. Rev. C, **4**, 1982 (1996).

12. R. Kunz et al., Phys. Rev. Let., **86** 3244 (2001).

13. L. Buchmann. Phys. Rev. C, **64** 022801 (2001).

14. D.R. Tilley, H.R. Weller and C.M. Cheves, Nucl. Phys. A, **564** 1 (1993).

15. F.C. Barker and T. Kajino, Aust. J. Phys., **44** 396 (1991).

16. R.J. Holt, H.E. Jackson, R.M. Laszewski, J.E. Monohan, and J.R. Specht, Phys. Rev. C, **18** 1962 (1978).

17. C.R. Brune, W.R. Geist, R.W. Kavanaugh, and K.D. Veal, Phys. Rev. Lett., **83** 4025 (1999).

18. T.R. Ophel, A.D. Frawley, P.B. Treacy, and K.H. Bray, Nucl. Phys. **A 273**, 397 (1976)

19. L. Gialanella, PhD thesis, Bochum (2000)

20. R. Plaga, H.W. Becker, A. Redder, C. Rolfs, and H.P. Trautvetter, Nucl. Phys. A, **465**, 291 (1987).

21. C.R. Brune, Phys. Rev. C, **64** 0055803 (2001).

22. K. Chadan and P. C. Sabatier. *Inverse Problems in Quantum Scattering Theory.* Springer, New York, 1977.

23. P. Descouvemont. Microscopic description of the ^{16}O spectrum in a multiconfigurational cluster model. *Nucl. Phys. A*, 470:309–327, 1987.

24. J. Escher and B. Jennings. One-body overlap functions, equations of motion and phenomenological potentials. *Phys. Rev. C*, 66:034313, 2002.

25. J.-M. Sparenberg. Deep *l*-independent potentials from supersymmetric inversion. *Phys. Rev. Lett.*, 85:2661–2664, 2000.

26. C. Barbieri, W. H. Dickhoff. Fadddeev treatment of long-range correlations and the one-hole spectral function of ^{16}O. *Phys. Rev. C*, 65:064313, 2000.

27. C. Barbieri. Self-consistent Green's function study of low-energy correlations in ^{16}O. *Ph.D thesis*, Washington Univ., August 2002. C. Barbieri, W. H. Dickhoff. In preparation

28. N. Michel, *et al.*. Gamow shell model description of neutron-rich nuclei. *Phys. Rev. Lett.*, 89:042501, 2002.

29. R. Id Betan, *et al.*. Two particle resonant states in a many-body mean field. *Phys. Rev. Lett.*, 89:042502, 2002.

30. D. Hutcheon et al., submitted to Nuclear Instruments Methods A, 2002

31. C. Rolfs, Nucl. Phys. A, **217**, 29 (1973)

Include publications in refereed journal over at least the previous 5 years.

1. A.C. Morton, J.C. Chow, J.D. King, R.N. Boyd, N.P.T. Bateman, L. Buchmann, J.M. D'Auria, T. Davinson, M. Dombsky, W. Galster, E. Gete, U. Giesen, C. Iliadis, K.P. Jackson, J. Powell, G. Roy, and A. Shotter, "Beta-delayed particle decay of ^{17}Ne", Nucl. Phys. A, 706 (2002) 15

2. C. Ruiz, F. Sarazin, L. Buchmann, T. Davinson, R.E. Azuma, A.A. Chen, B.R. Fulton, D. Groombridge, L. Ling, A. Murphy, J. Pearson, I. Roberts, A. Robinson, A.C. Shotter, P. Walden, and P.J. Woods, "Strong resonances in elastic scattering of radioactive ^{21}Na on protons", Phys. Rev. C (Rapid Communications), 65 (2002) 042801(R)

3. D. Anthony, L. Buchmann, P. Bergbusch, J.M. D'Auria, M. Dombsky, U. Giesen, K.P. Jackson, J.D. King, J. Powell, and F.C. Barker, "Beta Delayed Deuteron emission from ^{6}He", Phys. Rev. C, 65 (2002) 034310

4. P. Tischhauser, R.E. Azuma, L. Buchmann, R. Detwiler, U. Giesen, J. Görres, M. Heil, J. Hinnefeld, F. Käppeler, J.J. Kolata, H. Schatz, A. Shotter, E. Stech, S. Vouzoukas, and M. Wiescher," Elastic α-^{12} scattering and the ^{12}C$(\alpha,\gamma)^{16}$O $E2$ S-factor", Phys. Rev. Let., 88 (2002) 072501

5. A. Zyuzin, S.H. Park, L. Buchmann, K.R. Buckley, A.R. Junghans, E.C. Mohrmann, K.A. Snover, T.D. Steiger, and J. Vincent, "The fabrication of metallic ^{7}Be targets with a small diameter for ^{7}Be$(p,\gamma)^{8}$B measurements", Nucl. Instr. Meth. B, 187 (2002) 264

6. A.R. Junghans, E.C. Mohrmann, K.A. Snover, T.D. Steiger, E.G. Adelberger, J.M. Casandjian, H.E. Swanson, L. Buchmann, S.H. Park, A. Zyuzin, "^{7}Be$(p,\gamma)^{8}$B" astrophysical S-factor from precision cross section measurements", Phys. Rev. Let., 88 (2002) 041101

7. L. Buchmann, "Radiative cascade transitions and the ^{12}C$(\alpha,\gamma)^{16}$O $E2$ cross section to the ground state of ^{16}O", Phys. Rev. C., 64 022801(R) (2001)

8. N. Bateman, K. Abe, G. Ball, L. Buchmann, J. Chow, J.M.D'Auria, Y. Fuchi, C. Iliadis, H. Ishiyama, K.P. Jackson, S. Karataglidis, S. Kato, S. Kubono, K. Kumagai, M. Kurokawa, X. Liu, S. Michimasa, P. Strasser, and M.H. Tanaka, " Measurement of the ^{24}Mg$(p,t)^{22}$Mg reaction and implications for the ^{21}Na$(p,\gamma)^{22}$Mg stellar reaction rate", Phys. Rev. C, 63 (2001) 035803

9. L.Buchmann, E.Gete, J.C.Chow, J.D.King, and D.F. Measday, "The β-delayed particle decay of ^{9}C and the A-9, T=1/2 nuclear system; R-matrix fits, the A=9 nuclear system, and the stellar reaction rate of ^{4}He$(\alpha n,\gamma)^{9}$Be", Phys. Rev. C., 63 (2001) 034303

10. E.Gete, L.Buchmann, R.E.Azuma, D.Anthony, N.Bateman, J.C.Chow, J.M.D'Auria, M.Dombsky, U.Giesen, C.Illiadis, K.P.Jackson, J.D.King, D.F. Measday, and A.C.Morton, "The β-delayed particle decay of ^{9}C and the A-9, T=1/2 nuclear system; Experiment, data and phenomenological analysis", Phys. Rev. C., 61 (2000) 064310

11. A.Y.Zyuzin, L.R.Buchmann, J.S.Vincent, K.R.Buckley, N.O.Bateman, K.A.Snover, J.M.Csandjan, T.D.Steiger, E.G.Adelberger, and H.E.Swanson, "Metallic beryllium-7 target of small diameter". Nucl. Inst. Meth., A438 (1999) 109

12. E.G.Adelberger, S.A.Austin, J.N.Bahcall, A.B.Balantkin, G.Bertsch, G.Bognert, L.S.Brown, L.Buchmann, F.E.Cecil, A.E.Champagne, L. de Braeckeleer, C.A.Duba, S.E.Elliott, S.J. Freedman, M.Gai, C.Goldring, C.R.Gould, A.Cruzinov, W.C.Haxton, K.M. Hoeger, E.Henley, C.W.Johnson, M. Kamionskowski, R.W. Kavanaugh, S.E.Koonin, K.Kubodera, K.Langanke, T. Motobayashi, V, Pandharipande, P.Parker, R.G.H. Robertson, C.Rolfs, R.F. Sawyer, N.Shaviv, T.D.Shoppa, K.Snover, E.Swanson, R.E.Tribble, S. Turck-Chiene, and J.F. Wikerson, "Solar Fusion Rates", Rev. Mod. Phys., 70 (1998) 1265

13. J.Görres, J. Meißner, H.Schatz, E.Stech, P.Tischhauser, M.Wiescher, R.Harkewics, B.Sherrill, M.Steiner, D. Bazin, M.Hellström, D.J.Morrissey, R.N.Boys, L.Buchmann, D.H.Hartmann, J.D.Hinnefeld, "Lifetime of ^{44}Ti as probe of supernova models", Phys. Rev Lett. 80 (1998) 2554

14. J.C.Chow, A.C.Morton, R.E.Azuma, N.Bateman, R.N.Boyd, L.Buchmann, J.M.D'Auria, T.Davinson, M.Dombsky, W.Galster, E.Gete, U.Giesen, C.Iliadis, K.P.Jackson, J.D.King, G.Roy, T.Shoppa, and A.Shotter, "Three-particle break-up of the isobaric analogue state in ^{17}F", Phys. Rev. C 57, (1998) R475